Hydrol. Earth Syst. Sci. Discuss., 9, 13117–13154, 2012
www.hydrol-earth-syst-sci-discuss.net/9/13117/2012/
doi:10.5194/hessd-9-13117-2012

Hydrology and Earth System Sciences Discussions

Water storage change estimation from in situ shrinkage measurements of clay soils

B. te Brake[1], **M. J. van der Ploeg**[1], **and G. H. de Rooij**[2]

[1]Soil Physics and Land Management Group, Wageningen University, Droevendaalsesteeg 4, 6708 PB Wageningen, The Netherlands
[2]Soil Physics Department, Helmholtz Centre for Environmental Research, Theodor-Lieser-Straße 4, 06120 Halle (Saale), Germany

Received: 29 October 2012 – Accepted: 9 November 2012 – Published: 21 November 2012

Correspondence to: B. te Brake (bram.tebrake@wur.nl)

Published by Copernicus Publications on behalf of the European Geosciences Union.

Abstract

Water storage in the unsaturated zone is a major determinant of the hydrological behaviour of the soil, but methods to quantify soil water storage are limited. The objective of this study is to assess the applicability of clay soil surface elevation change measurements to estimate soil water storage changes. We measured moisture contents in soil aggregates by EC-5 sensors, and in volumes comprising multiple aggregates and intra-aggregates spaces by CS616 sensors. In a prolonged drying period, aggregate-scale storage change measurements revealed normal shrinkage for layers ≥ 30 cm depth, indicating volume loss equalled water loss. Shrinkage in a soil volume including multiple aggregates and voids was slightly less than normal, due to soil moisture variations in the profile and delayed drying of deeper soil layers upon lowering of the groundwater level. This resulted in shrinkage curve slopes of 0.89, 0.90 and 0.79 for the layers 0–60, 0–100 and 0–150 cm. Under a dynamic drying and wetting regime, shrinkage curve slopes ranged from 0.29 to 0.69 (EC-5) and 0.27 to 0.51 (CS616). Alternation of shrinkage and incomplete swelling resulted in an underestimation of volume change relatively to water storage change, due to hysteresis between swelling and shrinkage. Since the slope of the shrinkage relation depends on the drying regime, measurement scale and combined effect of different soil layers, shrinkage curves from laboratory tests on clay aggregates require suitable modifications for application to soil profiles. Then, the linear portion of the curve can help soil water storage estimation from soil surface elevation changes. These elevation changes might be measurable over larger extents by remote sensing.

1 Introduction

The soil moisture status of the unsaturated zone has a major impact on terrestrial water fluxes. The amount and distribution of soil moisture determines the actual soil water storage capacity and the partitioning of precipitation into surface runoff, evaporation,

HESSD
9, 13117–13154, 2012

transpiration, and groundwater recharge (Milly, 1994; Western et al., 1999; Robinson et al., 2008). Quantifying these water fluxes is often done through establishing the water balance of a control volume under consideration (e.g. unsaturated zone of the soil, catchment or continent). At large spatial (e.g. continental or regional) scales, approaches like simple bucket models (often with lumped storage variables) might be satisfactory to establish the water balance (Milly and Dunne, 1994; Farmer et al., 2003). At finer spatial scales, or to study short term water balance dynamics, a more detailed representation of variations in fluxes and state variables is required (Eagleson, 1978) and measurements of soil water content are needed for closing the water balance (Robinson et al., 2008).

Methods to quantify soil water storage at and beyond the field scale are limited. Water balance methods have limited potential to determine soil water storage, as it is even harder to determine the various fluxes into and from the soil profile. The accumulation of measurement errors can be profound (Gee and Hillel, 1988; De Vries and Simmers, 2002). Normally, soil water storage in situ is estimated from multiple soil water content measurements. Contact-based soil moisture sensors provide direct information with high frequency, but only on very small measurement volume compared to the soil body of interest. To improve spatial coverage wireless sensors networks appear promising (Cardell-Oliver et al., 2005; Bogena et al., 2010). Optimally designing these networks for non-scientific applications still requires further work (Vereecken et al., 2008), but efforts in multiple disciplines (e.g. hardware technology, signal transmission, sensor data collection, data management), have resulted in significant progress in recent years (e.g. Bogena et al., 2007, 2009, 2010; Yang et al., 2010; Zhang et al., 2011). Contact-free measurements of soil moisture (e.g. ground based, airborne or spaceborne remote sensing techniques or hydrogeophysical measurements like ground penetrating radar, GPR, and electromagnetic induction, EMI) can give information on larger spatial scales. The relatively low temporal resolution and complexity of data acquisition and processing of these measurements is a drawback. Besides, radiometer-operating remote sensing techniques, and to a smaller extent GPR, suffer from limited penetration

HESSD
9, 13117–13154, 2012

depth of the electromagnetic signal, resulting in a estimation of soil moisture content from the top few centimetres of the soil only. Other applicability issues for these methods are quantification of the dielectric permittivity – soil moisture relation and surface roughness ambiguity (Huisman et al., 2003; Lievens et al., 2011). Modelling attempts to derive the soil profile water content from remotely sensed surface soil moisture measurements have only been partly successful (Arya et al., 1983; Walker et al., 2001; Vereecken et al., 2008). Also techniques to assimilate remotely sensed near-surface soil moisture observations into hydrological models require more development to explore all acquired data to its fullest (Crow and Ryu, 2009; Liu et al., 2011; Draper et al., 2012).

The lack of fully applicable measurement techniques makes it desirable to develop an alternative methodology to measure soil profile water storage and subsequently quantify subsurface fluxes more accurately. A possibility to do so is to rely on relationships between soil water content and other, more easily and accurately measurable, variables to infer soil water storage from. Measuring change in total water stored in the soil rather than the vertical distribution of soil water is an acceptable simplification for many hydrological purposes. It has been long recognized that surface elevation changes of expansive clay soils could serve as an estimate for soil water storage change (Yule and Ritchie, 1980a,b; Bronswijk, 1991b; Cabidoche and Ozier-Lafontaine, 1995; Cabidoche and Voltz, 1995; Kirby et al., 2003). Water storage change in clay soils results in volume change of the soil matrix and the relation between water storage change and volume change can be accurately quantified under laboratory conditions (e.g. Stirk, 1954; Bronswijk and Evers-Vermeer, 1990; Braudeau et al., 1999; Cornelis et al., 2006), in lysimeters (e.g. Yule and Ritchie, 1980a; Bronswijk, 1991a; Mitchell and Van Genuchten, 1992) and in situ (e.g. Aitchison and Holmes, 1953; Bridge and Ross, 1984; Bronswijk, 1991b; Cabidoche and Ozier-Lafontaine, 1995; Kirby et al., 2003; Coquet et al., 1998). Therefore, volume change of clayey soils is an attractive proxy for water storage change.

HESSD
9, 13117–13154, 2012

The shrinkage characteristic curve quantifies the relation between volume and water content of clay aggregates (Fig. 1). Volume and water content of swelling and shrinking soils are conveniently expressed relative to the volume of solids in the soil matrix, resulting in dimensionless factors void ratio e and moisture ratio ϑ:

$$e = \frac{\text{Volume of pores}}{\text{Volume of solids}} \tag{1}$$

$$\vartheta = \frac{\text{Volume of water}}{\text{Volume of solids}} \tag{2}$$

During shrinkage of initially saturated clay aggregates, four shrinkage phases can be distinguished (Haines, 1923; Bronswijk and Evers-Vermeer, 1990), indicated in Fig. 1:

1. Structural shrinkage: when saturated soils or large samples start drying, stable water-filled inter-aggregate pores are emptied. Due to this, aggregates can get a somewhat denser packing, which leads to small volume changes, but no aggregate volume change occurs.

2. Normal shrinkage: water loss of soil aggregates is completely compensated by volume decrease. The aggregates remain saturated.

3. Residual shrinkage: due to the dense packing of soil particles, water loss exceeds the volume change of aggregates. Air enters the pores of the aggregates.

4. Zero shrinkage: the soil particles have reached their densest configuration. Aggregate volumes do not decrease any further. The water loss is equal to the increase of the air volume in the aggregates.

The actual magnitude of swelling and shrinkage of clay soils as a result of wetting and drying, largely depends on soil properties (e.g. clay content, clay mineralogy, soil structure, soil water composition, and cation exchange capacity) and environmental factors (e.g temperature, groundwater depth, and climatology) (Nelson and Miller, 1992;

HESSD
9, 13117–13154, 2012

Parker et al., 1977). Therefore, the shrinkage behaviour of the soil in a field situation is expected to differ from the shrinkage behaviour of small samples used to measure the soil shrinkage characteristic curve. According to Parker et al. (1977) sample (or strata) size is a factor influencing in situ shrinkage behaviour. Cornelis et al. (2006) compared shrinkage curves obtained from soil cores, sieved samples, and undisturbed soil clods and their results suggest that sample size and treatment also influences laboratory shrinkage measurements. Small samples will hardly experience structural shrinkage, since there will be no inter-aggregate pores in the measurement volume.

Another expected major difference in shrinkage behaviour between laboratory and in situ measurements is a difference in slope of the shrinkage curve. During normal shrinkage of aggregates under laboratory conditions this slope equals one, meaning that volume change equals water storage change. Volume change of a field soil however, can result from aggregate swell and shrinkage, and a change of packing of aggregates. If the packing of shrinking aggregates becomes more dense, the volume loss of the aggregates is compounded by a loss of the inter-aggregate pore volume. If this occurs, the volume loss in the soil is larger than the water loss from the soil, thereby yielding a shrinkage curve slope larger than one. According to Jayawardane and Greacen (1987) however, the shrinkage curve (and swelling curve) of a large volume of soil in the field (comprising multiple aggregates) will have a smaller slope due to development of cracks and presence of stable non-clayey soil particles. If soil water content change is measured on the same scale as volume change, and not only sampled in the soil volume between cracks, slopes close to unity might still be obtained.

A field soil under a variable regime including multiple drying and wetting cycles, may experience the effect of hysteresis between swelling and shrinkage. This was observed by Peng and Horn (2007) after gradual drying and re-wetting of small cores. They distinguished two distinct parts in the swelling curve: virgin swelling at first swelling, with slopes close to one, followed by residual swelling at further wetting, where the moisture ratio increased but hardly any swelling was observed. Wetting cycles during which the soil volume is not completely restored by swelling, will then result in an underestimation

HESSD
9, 13117–13154, 2012

of volume change with respect to soil water storage change, and the slope of the net resulting shrinkage curve will be smaller than one.

Bronswijk (1990) measured the shrinkage geometry of soil cores with and without overburden pressure and concluded that removing overburden pressure yields non-isotropic shrinkage, while including overburden pressure (as in a field situation) yields isotropic shrinkage over the soil moisture range from saturation to oven dryness. Chertkov (2005) found shrinkage geometry to vary with moisture content and shrinkage phase and reported dominance of vertical shrinkage over stretching (horizontal shrinkage) after development of relatively large cracks. This stage was preceded by a stage of isotropic shrinkage in which many thin cracks developed, of which only a part did develop into large cracks. Non-isotropic shrinkage, with dominance of horizontal crack development over vertical shrinkage caused by anchoring of soil to tap roots, was reported by Mitchell (1991) and Mitchell and Van Genuchten (1992).

The objective of this study is to asses the applicability of measurements of periodic vertical movement of the soil surface to estimate soil water storage changes in the field. If the relationship between these variables can be accurately quantified, it may provide a basis for upscaling soil water storage change estimates to the field or catchment scale. To do so, we establish the in situ relationship between soil water storage change from contact based sensors and soil volume change calculated from soil surface elevation changes. The effect of several factors is assessed: drying regime, measurement scale of soil moisture sensors, profile depth and texture variations in the soil profile.

2 Materials and methods

2.1 Site description

Field measurements of soil water content and vertical shrinkage were performed on two adjacent agricultural fields in the Purmer area, approximately 15 km north of Amsterdam, the Netherlands. The Purmer area is a polder of 27.55 km^2 with clay-rich soils

HESSD
9, 13117–13154, 2012

of marine origin, situated between 3 and 4.5 m below mean sea level. The area is artificially drained by three pumping stations to maintain water levels suitable for agriculture (grassland and crop rotation of mainly potatoes, maize, sugar beets, and wheat; in total 63 % of the area), urban land use (22 %) and forest/parks (12 %). Open water makes makes up 3 % of the total area. The Purmer and it's location in the Netherlands are shown in Fig. 2. Measurements were performed on two fields in the north of the area. On field A (crop: Kentucky Bluegrass for seed harvesting) measurements were taken from April 2010 until October 2011. On field B (sugar beets) measurements were taken between April 2010 and November 2010.

All soil layers in the upper 100 cm at field A were classified as loam (Table 1) (Soil Survey Staff, 2010). Below 100 cm a higher sand fraction was observed, but the exact grain size distribution was not determined. At field B the soil is clearly layered, with loam and sandy loam horizons in the upper 50 cm and loamy sand and sand horizons below (Table 1). The clay fraction consisted of 65 % montmorillonite, 25 % illite and 10 % kaolinite minerals, as determined by X-ray diffraction.

2.2 Swelling and shrinkage measurements

To measure surface elevation changes resulting from clay swelling and shrinkage, ground anchors were installed, based on a technique used by Bronswijk (1991b). The ground anchors consisted of metal rods with two 95 mm diameter discs at one end, of which one could rotate freely and one was attached to the rod. When a ground anchor was lowered in a 100 mm diameter auger hole it was fixed by rotating the rod, forcing both discs into the undisturbed sides of the hole. After refilling the hole, a triangular frame was placed over the rod, resting on the undisturbed soil around the refilled hole on three pins (Fig. 3). The length of the rod above the triangular frame, L (see Fig. 3), was measured between marked points on the triangular frame and at the top of the rod using a 0.01 mm accuracy digital calliper to record the change in thickness of the layer between the anchoring depth and the soil surface. In the following, the word "layer" refers to the soil slab between the soil surface and a given anchoring depth. Slabs of soil between two ground anchors are termed “layer increments”. Anchoring depths were 11, 19, 29, 56, 92 and 152 cm at field A and 7, 19, 27, 60, 95 and 157 cm at field B. For convenience we will refer to the targets depths of ground anchors (10, 20, 30, 60, 100 and 150 cm at each location) instead of exact layer thicknesses in the remainder of this paper. The measurement interval was mostly 11 days but ranged between 2 and 12 days for practical reasons. Cumulative thickness changes with respect to two reference days (15 May 2010 and 12 February 2011) were calculated.

2.3 Volume change

To calculate volume changes from layer thickness changes, information is needed on the shrinkage geometry of the soil layers. Shrinkage geometry is generally expressed by the dimensionless geometry factor r_s, after Rijnierse (1983). In case of isotropic shrinkage $r_s = 3$, while $1 < r_s < 3$ indicates dominance of vertical shrinkage over cracking and $r_s > 3$ indicates dominance of cracking over vertical shrinkage. Bronswijk (1991b) provided a set of equations that use r_s to convert vertical shrinkage measurements to soil water content changes, based on work by Aitchison and Holmes (1953) and Giraldez and Sposito (1983). Bronswijk (1990) found that $r_s \approx 3$ at in situ overburden pressure, and consequently he calculated volume change of the soil matrix by (Bronswijk, 1991b):

$$\Delta V = 3\Delta z - 3\frac{\Delta z^2}{z_s} + \frac{\Delta z^3}{{z_s}^2} \tag{3}$$

where ΔV is the soil volume change expressed per unit area, Δz is the vertical layer thickness change and z_s is the layer thickness at saturation, all in mm. We used Eq. (3) to convert the layer thickness changes to volume changes of the soil pedon (excluding the volume of the cracks). Values for z_s were substituted by $z(0)$, being the layer thicknesses at the reference day (either 15 May 2010 or 12 February 2011).

Bronswijk and Evers-Vermeer (1990) estimated that Dutch clay soils, under Dutch climatic conditions, mainly experience normal shrinkage, so for this situation ΔV equals water storage change ΔW. Including S for water loss in the structural shrinkage phase (Yule and Ritchie, 1980a) yields:

$$\Delta W = S + \Delta V \tag{4}$$

2.4 Soil moisture measurements

Volumetric soil moisture content was measured with two contact-based sensor types: EC-5 capacitance sensors (Decagon) and CS616 water content reflectometers (Campbell Scientific). Both sensors measure the dielectric permittivity of the soil, from which volumetric moisture content is calculated. The high frequency of 70 MHz at which both sensors are operating minimizes salinity and textural effects (Logsdon, 2009; Parsons and Bandaranayake, 2009; Francesca et al., 2010).

EC-5s have two flat, 1 × 5 × 56 mm pins spaced 5 mm apart, while CS616s have two 300 mm long rods with a diameter of 3.2 mm, spaced 32 mm apart. Measurement rods of CS616s are therefore almost 5 times longer and wider apart than those of EC-5s. As the measurement volume of EC-5s is restricted to the direct surroundings of the pins (Sakaki et al., 2008; Parsons and Bandaranayake, 2009), it is far smaller than the measurement volume the CS616s (Francesca et al., 2010).

The difference in measurement volume of the sensor types enabled us to study the relation between volume changes and soil water storage changes on two spatial scales. EC-5s were assumed to measure soil water content on aggregate and intra-aggregate pores scales, while CS616s measured soil water content over a larger volume including pores, larger cracks, structural pores and multiple aggregates (the bulk soil). Nine EC-5s were installed at 5, 7.5, 10, 22.5, 30, 45, 60, 80 and 100 cm depth, four CS616s at 7.5, 22.5, 45 and 80 cm depth. At field A, EC-5s were installed at 9 and 14 cm instead of 7.5 and 10 cm, and a CS616 was installed at 9 instead of 7.5 cm depth.

We relied on the manufacturer's calibration to derive soil moisture contents from dielectric measurements for both sensor types. A single standard calibration for all mineral soil types with electrical conductivity between 0.1 $\mathrm{dS\,m^{-1}}$ and 10 $\mathrm{dS\,m^{-1}}$ is provided

HESSD
9, 13117–13154, 2012

(Francesca et al., 2010; Decagon Devices, Inc., 2011). Kizito et al. (2008) suggest a soil specific calibration of EC-5s is not needed for mineral soils. For CS616s two calibration equations and a range of parameters are provided for mineral soils, depending on soil bulk density and soil salinity (Campbell Scientific, Inc., 2006). Of those, we found the quadratic equation with parameters based on a soil with relatively high bulk density and high soil salinity to provide the most realistic soil water contents, based on porosity and saturated water content measurements in the laboratory. Soil moisture content measurements were only used to calculate soil water storage change with respect to the reference days. It was expected that custom calibrations would not have a significant effect on soil water storage changes, which was corroborated by the subtle differences between the calculated changes in water storage based on the different calibration equations and parameter sets supplied by Campbell Scientific for the CS616.

The daily averaged soil moisture content per sensor was calculated for days at which layer thickness changes were measured. Soil water storage W was calculated twice for each layer, based on only EC-5 and only CS616 data, by assigning the mean soil moisture content of the closest sensor to any part of the layer under consideration. Because the thickness of the layers varied due to swelling and shrinkage, and W was calculated based on the initial depth d_i assigned to sensor i, we accounted for layer thickness change by the ratio between the actual layer thickness $z(t)$ and the initial layer thickness $z(0)$, f_{cor}:

$$W(t) = \sum_{i=1}^{n} \theta_i(t) d_i \cdot f_{\text{cor}} \tag{5}$$

with:

$$f_{\text{cor}} = \frac{z_l(t) - z_{l-1}(t)}{z_l(0) - z_{l-1}(0)} \tag{6}$$

In Eq. (5), n is the number of sensors used to calculate W, θ_i is the volumetric water content measured by sensor i and d_i is the depth assigned to this sensor. In Eq. (6),

HESSD
9, 13117–13154, 2012

l is the layer over which to calculate W and $l-1$ is the layer between surface level and the preceding ground anchor. For example, to obtain the correction factor for the layer increment 30–60 cm, l is 0–60 cm and $l-1$ is 0–30 cm. z_l and z_{l-1} denote the actual layer thicknesses at the time indicated in parentheses. Note that for the first layer (0–10 cm), z_{l-1} cancels out and f_{cor} is calculated from the ratio between actual layer thickness $z_{0-10}(t)$ and the initial layer thickness $z_{0-10}(0)$ only.

By applying this correction it was ensured that water storage in each sublayer was corrected proportionally to the thickness change of that sublayer and the correction was not lumped or averaged over the total layer under consideration. Soil water storage changes were then calculated with respect to the reference days. Due to sensor failures, the EC-5s at 45 cm and 100 cm at field A and the EC-5 at 45 cm at field B were not used in the calculations.

2.5 Groundwater level

Pressure transducers recorded groundwater levels in piezometers next to the ground anchors. One piezometer was installed at each measurement location at 22 July 2010. Atmospheric pressure was measured at field A to correct the measurements from the pressure transducers in the piezometers.

2.6 Meteorological data

2.6.1 Precipitation

The rainfall rate was measured by a Parsivel disdrometer (OTT Hydrometry Ltd, extensively described by Yuter et al., 2006), located approximately 150 m from the measurement location at field B and 300 m from the measurement location at field A. The disdrometer operated from June 2010 until October 2011, but due to datalogging problems, data between 7 July 2010 and 11 September 2010 were missing. Data gaps were filled with daily precipitation sums from the Royal Netherlands Meteorological Institute

HESSD
9, 13117–13154, 2012

(KNMI, 2012) precipitation station in Edam, located approximately 2.7 km north-east of the field site. As daily precipitation sums from KNMI stations were measured between 08:00 and 08:00 UTC, the disdrometer recordings with a frequency of one minute were summed over the same interval.

2.6.2 Potential evapotranspiration

Daily values of reference potential evapotranspiration from the KNMI weather station in Berkhout (ca. 16 km north of the field site) were used (KNMI, 2012). KNMI used a modified Makkink method for calculation of reference potential evapotranspiration (De Bruin, 1987; De Bruin and Lablans, 1998). Potential evapotranspiration for grass and sugar beets were calculated using crop coefficients provided per 10 day period by Feddes (1987). In the following, evapotranspiration is taken to mean potential evapotranspiration, unless stated differently.

3 Results and discussion

3.1 Drying regime, soil shrinkage, and groundwater depth in 2011

Spring 2011 was exceptionally drier, sunnier and warmer than average. KNMI reported the nation-wide averaged amount of precipitation (49 mm) in the months March, April and May to be the lowest in 100 yr. Also the total of sunshine hours (686 h) was the highest in 100 yr time and mean temperature (11 °C) was the second highest ever recorded. Figure 4 shows the effect of these exceptional weather conditions on net precipitation, soil layer thickness change, soil moisture content, and groundwater depth at field A for the 112 day period under consideration here (12 February until 3 June 2011).

The period was characterized by progressive net evapotranspiration under meteorological forcings and the onset of the growing season. Total precipitation recorded by the disdrometer was 63.9 mm. The precipitation event of late February had an substantial

HESSD
9, 13117–13154, 2012

effect on cumulative P-ET, since the evapotranspiration rate was still small at that time (Fig. 4a). Later events however, were rapidly compensated by high evapotranspiration rates, resulting in total cumulative P-ET of −174 mm at 3 June.

In February the soil was near saturation and the onset of the dry period at 28 February resulted in continuous shrinkage of the layers up to 60 cm between 7 March and 3 June Fig. 4b. The only exception is the layer 0–10 cm between 11 May and 23 May, where a negligible 0.02 mm swelling was observed. In the first interval between 12 February and 23 February no shrinkage was observed, but the layers 0–100 cm and 0–150 cm swelled up to 1 mm. Total cumulative vertical shrinkage at 3 June in the layers 0–10, 0–20, 0–30 and 0–60 cm was 8.4, 15.2, 16.4 and 21.3 mm. Shrinkage below 60 cm was negligible, as evidenced from the similarity of the curves below this depth. The layer increment between 30 and 60 cm started contributing significantly to total shrinkage at 19 April and shrinkage almost completely originated from this layer after 30 April.

At 1 May, the start of a decrease in soil moisture content (θ, CS616) at 45 cm depth was measured (Fig. 4c), gradually proceeding to the end of the measurement period. In the same period, θ measured by sensors installed shallower and deeper than 45 cm remained relatively constant. This coincided with the dominance of shrinkage in the between 30 to 60 cm layer increment. Small amounts of precipitation after 1 May did not increase the soil moisture content and no swell was measured.

Although the groundwater level declined from approx. 100 cm below surface level in early March to ca. 150 cm in June (Fig. 4c), moisture content at 80 cm did not change and no additional shrinkage was observed between 60 and 150 cm in this period. Around the time the groundwater level peaked in February however, the moisture content at 80 cm was changing abruptly. A time lag of about 4 days was observed between the decline of the groundwater level and soil moisture content. At the start of the soil moisture decline, the groundwater level was approx. 110 cm below surface level, indicating that the depth of the full-capillary zone above groundwater level was approx. 30 cm. Further lowering of the groundwater table and the capillary fringe caused

$0.055\,cm^3\,cm^{-3}$ moisture content change. Relatively large pores emptied, while the soil matrix retained water, leading to a stable moisture content above the capillary fringe. The observation of the depth and water content of the capillary fringe could be used to correct water storage change calculated from CS616 measurements. A similar correction was applied to the EC-5 data, although there was hardly any response of the aggregate-scale soil moisture content to groundwater fluctuations.

3.2 Volume change and soil water storage change of a field soil during extensive drying

Figure 5 shows the relation between volume change ΔV and soil water storage change ΔW in the six soil layers, from the two water content sensor types. For the soil layer extending from the soil surface to the capillary fringe, the ΔV–ΔW relationship represents the soil profile scale equivalent of void ratio and moisture ratio as used in the shrinkage curve of individual clay aggregates (Fig. 1). A linear relation ($\Delta V = a\Delta W + b$) was fitted through the data points representing volume change outside the structural shrinkage phase, meaning the first measurement interval was omitted, since no significant volume change was observed. The decrease in water storage during this interval therefore indicates water loss in the structural shrinkage phase S, while the slope a indicates the degree of normal shrinkage. The fitted slopes are given in Fig. 5, and all fitting parameters and goodness of fit R^2 are summarized in Table 2.

Water loss in the structural shrinkage phase increased with depth (Table 2) and was larger based on CS616 measurements than based on EC-5 measurements, consistent with the larger measurement volumes (comprising both aggregates and voids) of the CS616.

The fitted slopes based on CS616 measurements are always lower than those based on EC-5 measurements. All slopes are close to one, except the slopes based on EC-5 measurements for the upper two layers (> 1) and the slope based on CS616 measurements for the deepest layer (< 1). In the upper layers (0–10 and 0–20 cm), volume change was overestimated compared to soil water storage change from both sensor types. After an initial stage of considerable drying, during which shrinkage was close to normal until 28 March (slope between two successive data points (local slope) close to one), and less than normal until 12 April (local slope smaller than one; residual shrinkage), the local slope in the dry end was much larger than one. Relative overestimations of ΔV can result from a change of packing of aggregates or an overestimation of the geometry factor r_s. Chertkov (2005) reported a decrease of r_s to about 2 after development of relatively large cracks. If the packing of a soil is stable, but vertical shrinkage exceeds horizontal shrinkage ($1 < r_s < 3$), the calculated volume loss will be overestimated by using Eq. (3) and the shrinkage curve slope will be larger than one. Until March 28 (before the slope of the shrinkage relation changed) we only observed small cracks in the soil surface (width ≤ 5 mm). From April 30 onwards (after the change in the slope), the cracks were much wider (≥ 10 mm). The commensurate change in crack width and soil profile shrinkage curve slope is consistent with the change in the geometry factor reported by Chertkov (2005). To fully explain the overestimation of ΔV, r_s should have been as low as 1.4 for the 0–10 cm layer in the dry range. The succession of normal and residual shrinkage and apparent changes in r_s with moisture content, still resulted in a fitted slope close to one for water storage change based on CS616 measurements in the upper layers.

During continuous drying, the EC-5 sensor captured soil moisture changes in aggregates that correlate with normal shrinkage, as evidenced from the slope close to one for layers deeper than 20 cm. In the dry end of the normal shrinkage phase, local slopes based on EC-5 measurements slightly exceeded one, occasionally resulting in a fitted slope a larger than one. This is an effect of the overestimation of ΔV in the upper layers.

In general, shrinkage was close to normal for layers of 30 cm or deeper for EC-5 sensors. The CS616 sensors trended towards smaller slopes with depth, but were still close to one for the 0–60, 0–100 and 0–150 cm layers (Fig. 5). In the penultimate measurement interval (between 11 May and 23 May), the volume change was only 2.2, 2.0, 4.1 and 2.5 mm in the layers 0–30, 0–60, 0–100 and 0–150 cm, while soil water storage change (CS616) in these layers declined with 1.6, 9.0, 10.8 and 12.6 mm. The lower soil layers drained water stored in large pores to the lowered groundwater level (see Fig. 4c), which resulted in little shrinkage below 30 cm depth, but a rapid decrease in water storage. In the final measurement interval the local slopes for the layers 0–60, 0–100 and 0–150 cm had increased again to 0.96, 0.73 and 0.67. Large soil moisture content differences in the profile – caused by delayed drying of the lower layers and large influence of the capillary fringe – led to this kind of shrinkage behaviour. The fitted slope of the shrinkage curve of the deepest soil layers resulted from zero-shrinkage of the upper part of the soil, structural shrinkage of the lower part and residual shrinkage in the layers in between, compounded by r_s changes upon drying in the upper layers. Similar findings were reported by Yule and Ritchie (1980a,b) for small and large cores. Yule and Ritchie (1980b) suggested that simultaneous water loss from multiple depths in a profile may stem from the structural and (normal) shrinkage phase until most of the plant available water has been used.

3.3 Drying regime, soil shrinkage, and groundwater depth in 2010

The growing season of 2010 offered a more dynamic precipitation and evapotranspiration regime, with both dry and wet periods, and measurements were performed on a field with a lower clay content (field B). The season was characterized by two periods of progressive drying, between 15 May and 8 June and between 11 June and 5 August, and a wet period after 5 August (Fig. 6a). The periods of net drying were separated by extensive rainfall (49.1 mm) on 9 and 10 June, resulting in swelling measured in all layers at 15 June (Fig. 6b). The second drying period included three days with a total rainfall of 69.6 mm in mid July. After 5 August, precipitation events were frequent and large, with a precipitation sum of 226 mm in August, while the 30-yr mean total precipitation sum in August was 90 mm.

At the start of the measurement period the soil was near saturation and soil layer thickness at the end of the measurement period was almost completely recovered to

HESSD
9, 13117–13154, 2012

the level at the start. Between 15 June and 26 June, shrinkage of the 0–60 cm layer was larger than shrinkage of deeper layers. This might have been a measurement error, since the magnitudes and patterns of thickness variations were comparable for the 0–30, 0–60 and 0–100 cm layers for other intervals. Therefore most volume change resulted from the upper 30 cm of the soil (Fig. 6b), although soil moisture content at 45 cm did decrease considerably between early July and early August. Thickness change due to swelling and shrinkage below 50 cm depth was expected to be small, because clay content is maximum 5.9 % (Table 1).

Swelling of all layers between 0 and 100 cm was observed at 13 July and 18 July, caused by heavy rainfall in mid July, but hardly any swelling of the layer 0–150 cm was observed. Also soil moisture content increased at 7.5, 22.5 and 45 cm depth, while soil moisture content at 80 cm decreased slightly. EC-5s at 80 and 100 cm also decreased in this period (results not shown). Apparently, the layer increment 100–150 cm shrank, counteracting the swelling of the layer 0–100 cm. Shrinkage of the soil above 100 cm after 18 July, resulted in maximum total vertical shrinkage of 11.6 mm at 29 July.

The contribution of groundwater storage change to ΔW could not be considered for 2010, since groundwater level measurements only started at 22 July. Also, the soil moisture content did not exhibit a clear response to groundwater level variations, so the extent of the capillary fringe could not be estimated (Fig. 6b). The layer thickness changes and slowly rising groundwater level after substantial rainfall in early August showed that water was stored in the soil. From late August, when swelling was nearly complete and the soil was near saturation, groundwater level reacted rapidly to precipitation. The very slow recovery of layer thickness after late August corresponds to observations of swelling curves by Peng and Horn (2007) of rapid swelling at first rewetting, followed by residual swelling at further wetting, when the moisture ratio increased but hardly any swelling was observed.

HESSD
9, 13117–13154, 2012

3.4 Relation between volume change and soil water storage change in 2010

The dynamical regime of precipitation and evapotranspiration caused alternating swelling and shrinkage periods and variation in soil water storage change with respect to the starting date. Water loss in the structural shrinkage phase could not objectively be distinguished, due to scatter of the relation storage change and volume change, partly caused by residual swelling from September to November. Maximum soil volume was expected to occur in the structural shrinkage phase and a linear relation relation ($\Delta V = a\Delta W + b$) was fitted through all datapoints with water storage smaller than water storage at maximum volume (Fig. 7). By applying this procedure, the number of points fitting is based on can vary between layers and sensors. Fitting parameters and goodness of fit R^2 are summarized in Table 3.

There is a mismatch between the response of water storage change based on EC-5s and volume change, at least at the measurement frequency and scale used here. In case of swelling, the expected change in water storage was often not observed (Fig. 7). Hysteresis between swelling and shrinkage was also observed by Peng and Horn (2007). Since swelling was incomplete at all times (i.e. the soil did not return to its maximal volume), the net water storage change was larger than net volume change, resulting in mild slopes. The effect of variable conditions, with alternation of shrinkage and swelling was enhanced by a difference in measurement scale of soil surface elevation change by ground anchors and soil moisture content by EC-5 sensors. Soil water content and volume change mainly occurred in parts of the soil that were in close contact with the atmosphere (e.g. the top of the soil and inter-aggregate pores), and less from the interior of aggregates in which the EC-5s were measuring. The small measurement volumes of EC-5s were thus relatively shielded from water content changes, and not representative for the profile-scale at which the volume change measurements were acquired. The measurement scale of the CS616s (including aggregates and inter-aggregate spaces) matched better with the scale of volume change measurements,

HESSD
9, 13117–13154, 2012

resulting in less scatter for soil water storage change based on CS616 measurements, slightly higher R^2 values (Table 3), and no hysteresis in the dry range.

Soil water storage changes calculated from the CS616s were larger than those calculated from EC-5s, and the slopes were larger for EC-5 data than for CS616 data, except for the layer 0–150 cm (which will be discussed below). Larger slopes indicate a larger volume change per unit storage change. Volume change based on EC-5 measurements is thus closer to normal, which can be expected from the aggregate-scale of the measurements.

Slopes vary considerably with depth. In the upper layers slopes are low, probably because the effect of alternating occurrence of swelling and shrinkage is largest here. This effect is less in deeper layers and the largest slopes for both soil moisture sensors are observed in the layers 0–30 and 0–60 cm. In the sandy layers below 50 cm, little volume change will occur upon water storage change, resulting in small slopes in the layers 0–100 and 0–150 cm.

The clay content in the upper 50 cm is comparable to field A, so slopes approaching one would be expected during uninterrupted shrinkage. If only the datapoints representing shrinkage were considered, slopes based on EC-5 measurements for the layers 0–30 and 0–60 were 0.80 and 0.81. This indicated close to normal shrinkage, but slopes were deviating from one because volume change and water storage change were the net result of water storage variations in the interval between shrinkage points. Shrinkage slopes for other layers were lower. The relatively mild slopes (less-than-normal shrinkage) can be regarded as the net result of no shrinkage of rigid soil particles and reduced (residual or zero) shrinkage of dry surface layers of aggregates combined with normal shrinkage in the clay aggregates interiors (Yule and Ritchie, 1980a,b). The variation in shrinkage stages within a soil layer can safely be assumed to have been caused and/or enhanced by the changes in weather forcings (precipitation, temperature, solar radiation) as observed in 2010.

The relatively large slope for the 0–150 cm layer based on CS616 measurements is striking. Since no groundwater storage change estimation could be made, water storage change in this layer was largely determined by moisture content changes in the CS616 sensor installed at 80 cm depth. Moisture contents measured by the EC-5 and CS616 at this depth varied only slightly in the dry periods. The EC-5 at 100 cm however, recorded a considerable moisture content decrease, resulting in relatively large water storage change based on EC-5 measurements in the 0–150 cm layer. The four CS616 sensors may therefore have underestimated the water storage change in the 0–150 cm layer, thereby overestimating the slope in the ΔV–ΔW relationship. Preferred root water uptake by sugar beets from deep layers, as reported by Brown et al. (1987) and Camposeo and Rubino (2003) might be an explanation for water content changes at 100 cm depth.

4 Conclusions and outlook

Normal shrinkage is the major shrinkage phase in a clayey field soil under continuous drying, on both aggregate scale and bulk soil scale, including inter-aggregate pores, cracks, structural pores, and multiple aggregates. This confirms the conclusion by Bronswijk (1990) that clay soils under Dutch climatic conditions mainly experience normal isotropic shrinkage. At the bulk soil scale, the structural shrinkage phase accounts for a large share of water loss of the profile. Deep layers may remain wet for a long time, under influence of the ground water level and moisture content in the capillary fringe. At first drying these deeper layers will experience structural shrinkage, while the drier upper soil experiences normal, residual or zero shrinkage, causing the net shrinkage of the entire soil profile to be less than normal. Textural layering, soil moisture content gradients, and groundwater level are therefore important factors determining total soil-profile volume change and its relation with soil water storage change.

Different relations between soil water storage change and volume change at different measurement scales are enhanced by a variable wetting and drying regime. Hysteresis between swelling and drying enhances the effect of soil layers experiencing different

HESSD
9, 13117–13154, 2012

shrinking phases, thereby further lowering shrinkage curve slopes. The relation between soil water storage change and volume change remains linear and soil moisture measurements in large soil volumes (spanning multiple aggregates and cracks) are relatively robust.

Due to the linearity of the relationship between storage change and soil volume change and the validity of the assumption of isotropic shrinkage, measurements of surface level elevation changes can potentially be used to estimate soil water storage change of the entire soil profile. The effect of variable drying and wetting conditions has to be considered however, since solely relying on surface level elevation changes will lead to an underestimation of soil water storage variations. Detailed knowledge on the shrinkage geometry factor variation with soil moisture content may improve soil water storage estimations if shrinkage is outside the normal shrinkage range.

We showed that in very dry conditions for Dutch standards, the potential overestimation of volume change is limited and negligible if a deep soil layer (the entire soil profile) is considered. Current and future technologies like GPS, satellite or airborne radar interferometry (InSAR), and airborne laser scanning (LIDAR) may be capable of measuring elevation changes with sufficient vertical and temporal detail on larger (field to catchment) scales, so that water storage changes in soil profiles on these larger scales can be inferred (Gabriel et al., 1989; Bamler and Hartl, 1998; Gao, 2007; Te Brake et al., 2012). Since the slope of the relationship between water storage change and volume change (in situ shrinkage curve) depends on the drying regime and measurement scale, direct translation of shrinkage curves obtained through conventional laboratory tests on clay aggregates needs to be applied with care; at this time it is still better to directly observe the in situ shrinkage curves rather than convert a laboratory curve to field conditions. Such field-scale swelling and shrinkage curves need only be determined once for a given location, but require weather conditions that allow the soil to go through a wide range of water contents and alternating swelling and shrinkage.

HESSD
9, 13117–13154, 2012

Title Page
Abstract Introduction
Conclusions References
Tables Figures
◀ ▶
Back Close
Full Screen / Esc
Printer-friendly Version
Interactive Discussion

Acknowledgements. The authors thank Dirk and Jan de Heer and Roland Knook for kindly permitting access to the measurement locations and for support during the field campaign. Meteorological data, except for Parsival data, were provided by the Royal Netherlands Meteorological Institute. Technical support was provided by Harm Gooren, Hennie Gertsen and Pieter Hazenberg from Wageningen University. This research was financially supported by Netherlands Space Office (NSO) under project GO-AO/12.

References

Aitchison, G. and Holmes, J.: Aspects of swelling in the soil profile, Aust. J. App. Sci., 4, 244–259, 1953. 13120, 13125

Arya, L. M., Richter, J. C., and Paris, J. F.: Estimating profile water storage from surface zone soil-moisture measurements under bare field conditions, Water Resour. Res., 19, 403–412, 1983. 13120

Bamler, R. and Hartl, P.: Synthetic aperture radar interferometry, Inverse Probl., 14, R1–R54, doi:10.1088/0266-5611/14/4/001, 1998. 13138

Bogena, H. R., Huisman, J. A., Oberdoerster, C., and Vereecken, H.: Evaluation of a low-cost soil water content sensor for wireless network applications, J. Hydrol., 344, 32–42, doi:10.1016/j.jhydrol.2007.06.032, 2007. 13119

Bogena, H. R., Huisman, J. A., Meier, H., Rosenbaum, U., and Weuthen, A.: Hybrid wireless underground sensor networks: quantification of signal attenuation in soil, Vadose Zone J., 8, 755–761, doi:10.2136/vzj2008.0138, 2009. 13119

Bogena, H. R., Herbst, M., Huisman, J. A., Rosenbaum, U., Weuthen, A., and Vereecken, H.: Potential of wireless sensor networks for measuring soil water content variability, Vadose Zone J., 9, 1002–1013, doi:10.2136/vzj2009.0173, 2010. 13119

Braudeau, E., Costantini, J. M., Bellier, G., and Colleuille, H.: New device and method for soil shrinkage curve measurement and characterization, Soil Sci. Soc. Am. J., 63, 525–535, 1999. 13120

Bridge, B. J. and Ross, P. J.: Relations among physical properties of cracking clay soils, in: Properties and Utilisation of Cracking Clay Soils, edited by: McGarity, J. W., Hoult, E. H., and So, H. B., University of New England: Armidale, New South Wales, Australia, 97–104, 1984. 13120

Bronswijk, J. J. B.: Shrinkage geometry of a heavy clay soil at various stresses, Soil Sci. Soc. Am. J., 54, 1500–1502, 1990. 13123, 13125

Bronswijk, J. J. B.: Drying, cracking, and subsidence of a clay soil in a lysimeter, Soil Sci., 152, 92–99, 1991a. 13120

Bronswijk, J. J. B.: Relation between vertical soil movements and water-content changes in cracking clays, Soil Sci. Soc. Am. J., 55, 1220–1226, 1991b. 13120, 13124, 13125

Bronswijk, J. J. B. and Evers-Vermeer, J. J.: Shrinkage of Dutch clay soil aggregates, Neth. J. Agr. Sci., 38, 175–194, 1990. 13120, 13121, 13125

Brown, K., Messem, A., Dunham, R., and Biscoe, P.: Effect of drought on growth and water-use of sugar-beet, J. Agr. Sci., 109, 421–435, 1987. 13137

Cabidoche, Y. M. and Ozier-Lafontaine, H. O.: Theresa 1: matric water-content measurements through-thickness variations in vertisols, Agr. Water Manage., 28, 133–147, 1995. 13120

Cabidoche, Y. M. and Voltz, M.: Nonuniform volume and water-content changes in swelling clay soil. 2: A field-study on a vertisol., Eur. J. Soil Sci., 46, 345–355, 1995. 13120

Campbell Scientific, Inc.: CS616 and CS625 Water Content Reflectometers, Instruction manual, Revision, 8/06, 2006. 13127

Camposeo, S. and Rubino, P.: Effect of irrigation frequency on root water uptake in sugar beet, Plant Soil, 253, 301–309, doi:10.1023/A:1024801312711, 2003. 13137

Cardell-Oliver, R., Kranz, M., Smettem, K., and Mayer, K.: A reactive soil moisture sensor network: Design and field evaluation, in: International Conference on Intelligent Sensing and Sensor Networks, Melbourne, Australia, December 2004, 149–162, doi:10.1080/15501320590966422, 2005. 13119

Chertkov, V. Y.: The shrinkage geometry factor of a soil layer, Soil Sci. Soc. Am. J., 69, 1671–1683, 2005. 13123, 13132

Coquet, Y., Touma, J., and Boivin, P.: Comparison of soil linear shrinkage curve from extracted cores and in situ, Aust. J. Soil Res., 36, 765–782, 1998. 13120

Cornelis, W. M., Corluy, J., Medina, H., Díaz, J., Hartmann, R., Van Meirvenne, M., and Ruiz, M. E.: Measuring and modelling the soil shrinkage characteristic curve, Geoderma, 137, 179–191, doi:10.1016/j.geoderma.2006.08.022, 2006. 13120, 13122

Crow, W. T. and Ryu, D.: A new data assimilation approach for improving runoff prediction using remotely-sensed soil moisture retrievals, Hydrol. Earth Syst. Sci., 13, 1–16, doi:10.5194/hess-13-1-2009, 2009. 13120

De Bruin, H.: From Penman to Makkink, in: Evaporation and Weather, edited by: Hooghart, J. C., Proceedings and information No. 39, Comm. Hydrol. Res. TNO, Den Haag, 5–31, 1987. 13129

De Bruin, H. and Lablans, W.: Reference crop evapotranspiration determined with a modified Makkink equation, Hydrol. Process., 12, 1053–1062, doi:10.1002/(SICI)1099-1085(19980615)12:7<1053::AID-HYP639>3.0.CO;2-E, 1998. 13129

De Vries, J. J. and Simmers, I.: Groundwater recharge: an overview of processes and challenges, Hydrogeol. J., 10, 5–17, 2002. 13119

Decagon Devices, Inc.: Calibration Equations for the ECH2O EC-5, ECH2O-TE and 5TE Sensors, Tech. rep., 2011. 13127

Draper, C. S., Reichle, R. H., De Lannoy, G. J. M., and Liu, Q.: Assimilation of passive and active microwave soil moisture retrievals, Geophys. Res. Lett., 39, L04401, doi:10.1029/2011GL050655, 2012. 13120

Eagleson, P. S.: Climate, soil, and vegetation. 6. Dynamics of the annual water balance, Water Resour. Res., 14, 749–764, 1978. 13119

Farmer, D., Sivapalan, M., and Jothityangkoon, C.: Climate, soil, and vegetation controls upon the variability of water balance in temperate and semiarid landscapes: downward approach to water balance analysis, Water Resour. Res., 39, 1035, doi:10.1029/2001WR000328, 2003. 13119

Feddes, R.: Crop factors in relation to Makkink's reference crop evapotranspiration, in: Evaporation and Weather, edited by: Hooghart, J. C., Proceedings and information No. 39, Comm. Hydrol. Res. TNO, Den Haag, 33–45, 1987. 13129

Francesca, V., Osvaldo, F., Stefano, P., and Paola, R. P.: Soil Moisture Measurements: Comparison of instrumentation performances, J. Irrig. Drain. E.-ASCE, 136, 81–89, 2010. 13126, 13127

Gabriel, A., Goldstein, R., and Zebker, H.: Mapping small elevation changes over large areas – differential radar interferometry, J. Geophys. Res.-Solid, 94, 9183–9191, doi:10.1029/JB094iB07p09183, 1989. 13138

Gao, J.: Towards accurate determination of surface height using modern geoinformattic methods: possibilities and limitations, Prog. Phys. Geog., 31, 591–605, doi:10.1177/0309133307087084, 2007. 13138

Gee, G. W. and Hillel, D.: Groundwater recharge in arid regions – review and critique of estimation methods, Hydrol. Process., 2, 255–266, 1988. 13119

HESSD

9, 13117–13154, 2012

Giraldez, J. and Sposito, G.: A general soil volume change equation: 2. Effect of load pressure, Soil Sci. Soc. Am. J., 47, 422–425, 1983. 13125
Haines, W.: The volume-changes associated with variations of water content in soil, J. Agr. Sci., 13, 296–310, doi:10.1017/S0021859600003580, 1923. 13121
Huisman, J. A., Hubbard, S. S., Redman, J. D., and Annan, A. P.: Measuring soil water content with ground penetrating radar: a review, Vadose Zone J., 2, 476–491, 2003. 13120
Jayawardane, N. S. and Greacen, E. L.: The nature of swelling in soils, Aust. J. Soil Res., 25, 107–113, 1987. 13122
Kirby, J. M., Bernardi, A. L., Ringrose-Voase, A. J., Young, R., and Rose, H.: Field swelling, shrinking, and water content change in a heavy clay soil, Aust. J. Soil Res., 41, 963–978, 2003. 13120
Kizito, F., Campbell, C. S., Campbell, G. S., Cobos, D. R., Teare, B. L., Carter, B., and Hopmans, J. W.: Frequency, electrical conductivity and temperature analysis of a low-cost capacitance soil moisture sensor, J. Hydrol., 352, 367–378, doi:10.1016/j.jhydrol.2008.01.021, 2008. 13127
KNMI: available at: http://www.knmi.nl, last access: 26 September 2012. 13129
Lievens, H., Verhoest, N. E. C., De Keyser, E., Vernieuwe, H., Matgen, P., Álvarez-Mozos, J., and De Baets, B.: Effective roughness modelling as a tool for soil moisture retrieval from C- and L-band SAR, Hydrol. Earth Syst. Sci., 15, 151–162, doi:10.5194/hess-15-151-2011, 2011. 13120
Liu, Q., Reichle, R. H., Bindlish, R., Cosh, M. H., Crow, W. T., de Jeu, R., De Lannoy, G. J. M., Huffman, G. J., and Jackson, T. J.: The contributions of precipitation and soil moisture observations to the skill of soil moisture estimates in a land data assimilation system, J. Meteorol, 12, 750–765, doi:10.1175/JHM-D-10-05000.1, 2011. 13120
Logsdon, S. D.: CS616 Calibration: field versus laboratory, Soil Sci. Soc. Am. J., 73, 1–6, doi:10.2136/sssaj2008.0146, 2009. 13126
Milly, P. C. D.: Climate, interseasonal storage of soil-water, and the annual water-balance, Adv. Water Resour., 17, 19–24, 1994. 13119
Milly, P. C. D. and Dunne, K. A.: Sensitivity of the global water cycle to the water holding capacity of land, J. Climate, 7, 506–526, 1994. 13119
Mitchell, A. R.: Soil surface shrinkage to estimate profile soil-water, Irrigation Sci., 12, 1–6, 1991. 13123

Mitchell, A. R. and Van Genuchten, M. T.: Shrinkage of bare and cultivated soil, Soil Sci. Soc. Am. J., 56, 1036–1042, 1992. 13120, 13123

Nelson, J. and Miller, D.: Expansive Soils: Problems and Practice in Foundation and Pavement Engineering, Wiley, New York, 1992. 13121

Parker, J. C., Amos, D. F., and Kaster, D. L.: Evaluation of several methods of estimating soil volume change, Soil Sci. Soc. Am. J., 41, 1059–1064, 1977. 13122

Parsons, L. R. and Bandaranayake, W. M.: Performance of a new capacitance soil moisture probe in a sandy soil, Soil Sci. Soc. Am. J., 73, 1378–1385, doi:10.2136/sssaj2008.0264, 2009. 13126

Peng, X. and Horn, R.: Anisotropic shrinkage and swelling of some organic and inorganic soils, Eur. J. Soil Sci., 58, 98–107, doi:10.1111/j.1365-2389.2006.00808.x, 2007. 13122, 13134, 13135

Rijniersce, K.: A simulation model for physical soil ripening in the IJsselmeerpolders, Flevobericht No. 233, Rijksdienst voor de IJsselmeerpolders, Lelystad, 1983. 13125

Robinson, D. A., Campbell, C. S., Hopmans, J. W., Hornbuckle, B. K., Jones, S. B., Knight, R., Ogden, F., Selker, J., and Wendroth, O.: Soil moisture measurement for ecological and hydrological watershed-scale observatories: a review, Vadose Zone J., 7, 358–389, doi:10.2136/vzj2007.0143, 2008. 13119

Sakaki, T., Limsuwat, A., Smits, K. M., and Illangasekare, T. H.: Empirical two-point alpha-mixing model for calibrating the ECH2O EC-5 soil moisture sensor in sands, Water Resour. Res., 44, 526–531, doi:10.1029/2008WR006870, 2008. 13126

Soil Survey Staff: Keys to Soil Taxonomy, USDA-Natural Resources Conservation Service, Washington, DC, 11 Edn., 2010. 13124

Stirk, G. B.: Some aspects of soil shrinkage and the effect of cracking upon water entry into the soil, Aust. J. Agr. Res., 5, 279–290, 1954. 13120

Te Brake, B., Hanssen, R., Van der Ploeg, M., and De Rooij, G.: Satellite based radar interferometry to estimate large-scale soil water depletion from clay shrinkage: possibilities and limitations, Vadose Zone J., submitted, 2012. 13138

Vereecken, H., Huisman, J. A., Bogena, H., Vanderborght, J., Vrugt, J. A., and Hopmans, J. W.: On the value of soil moisture measurements in vadose zone hydrology: a review, Water Resour. Res., 44, W00D06, doi:10.1029/2008WR006829, 2008. 13119, 13120

Walker, J., Willgoose, G., and Kalma, J.: One-dimensional soil moisture profile retrieval by assimilation of near-surface observations: a comparison of retrieval algorithms, Adv. Water Resour., 24, 631–650, doi:10.1016/S0309-1708(00)00043-9, 2001. 13120

Western, A. W., Grayson, R. B., and Green, T. R.: The Tarrawarra project: high resolution spatial measurement, modelling and analysis of soil moisture and hydrological response, Hydrol. Process., 13, 633–652, 1999. 13119

Yang, J., Zhang, C., Li, X., Huang, Y., Fu, S., and Acevedo, M. F.: Integration of wireless sensor networks in environmental monitoring cyber infrastructure, Wirel. Netw., 16, 1091–1108, doi:10.1007/s11276-009-0190-1, 2010. 13119

Yule, D. F. and Ritchie, J. T.: Soil shrinkage relationships of Texas vertisols: 1. Small cores, Soil Sci. Soc. Am. J., 44, 1285–1291, 1980a. 13120, 13126, 13133, 13136

Yule, D. F. and Ritchie, J. T.: Soil shrinkage relationships of Texas vertisols: 2. Large cores, Soil Sci. Soc. Am. J., 44, 1291–1295, 1980b. 13120, 13133, 13136

Yuter, S. E., Kingsmill, D. E., Nance, L. B., and Loeffler-Mang, M.: Observations of precipitation size and fall speed characteristics within coexisting rain and wet snow, J. Appl. Meteorol. Clim., 45, 1450–1464, doi:10.1175/JAM2406.1, 2006. 13128

Zhang, R.-B., Guo, J.-J., Zhang, L., Zhang, Y.-C., Wang, L.-H., and Wang, Q.: A calibration method of detecting soil water content based on the information-sharing in wireless sensor network, Comput. Electron. Agr., 76, 161–168, doi:10.1016/j.compag.2011.01.010, 2011. 13119

HESSD

9, 13117–13154, 2012

Table 1. Grain size distribution at several depths of soils at field A and B.

Depth (cm)	Field A < 2 µm (%)	Field A 2–16 µm (%)	Field A 16–50 µm (%)	Field A > 50 µm (%)	Field B < 2 µm (%)	Field B 2–16 µm (%)	Field B 16–50 µm (%)	Field B > 50 µm (%)
0–15	19.0	40.1	20.8	21.1	19.2	39.1	22.1	19.6
15–30	18.0	35.1	23.5	23.4	15.2	28.4	23.8	32.6
30–50	19.8	34.8	22.7	22.7	15.4	29.5	21.4	33.7
50–70	18.2	33.9	21.7	26.2	5.9	8.9	9.4	75.8
70–90	23.6	43.2	24.2	9.0	–	–	–	–
90–100	18.9	35.6	19.1	26.4	3.4	4.8	6.5	85.3

HESSD
9, 13117–13154, 2012

Table 2. Fitted parameters for cumulative volume change outside the structural shrinkage phase, where $\Delta V = a\Delta W + b$, correlation coefficients between fit and observations, and observed water loss in the structural shrinkage phase S_{obs} for 2011.

Sensor	Layer (cm)	a	b	R^2	S_{obs} (mm)
EC-5	0–10	1.30	4.56	0.94	1.7
	0–20	1.26	7.66	0.88	2.9
	0–30	0.99	5.17	0.98	2.1
	0–60	1.13	20.90	0.95	14.6
	0–100	1.03	26.76	0.95	22.3
	0–150	0.97	25.25	0.97	22.9
CS616	0–10	0.99	3.77	0.95	3.4
	0–20	1.05	7.36	0.90	6.4
	0–30	0.86	9.23	0.95	11.1
	0–60	0.89	11.41	0.97	15.9
	0–100	0.90	27.15	0.96	34.7
	0–150	0.79	26.56	0.95	39.8

HESSD

9, 13117–13154, 2012

Table 3. Fitted parameters for cumulative volume change outside the structural shrinkage phase, where $\Delta V = a\Delta W + b$, and correlation coefficients between fit and observations, for 2010.

Sensor	Layer (cm)	a	b	R^2
EC-5	0–10	0.29	0.40	0.15
	0–20	0.37	−1.93	0.80
	0–30	0.66	−5.12	0.89
	0–60	0.69	−7.98	0.84
	0–100	0.42	−7.72	0.90
	0–150	0.37	−12.26	0.91
CS616	0–10	0.27	1.02	0.41
	0–20	0.32	0.60	0.82
	0–30	0.50	0.01	0.89
	0–60	0.51	−0.49	0.90
	0–100	0.36	−4.46	0.90
	0–150	0.48	−5.96	0.93

HESSD
9, 13117–13154, 2012

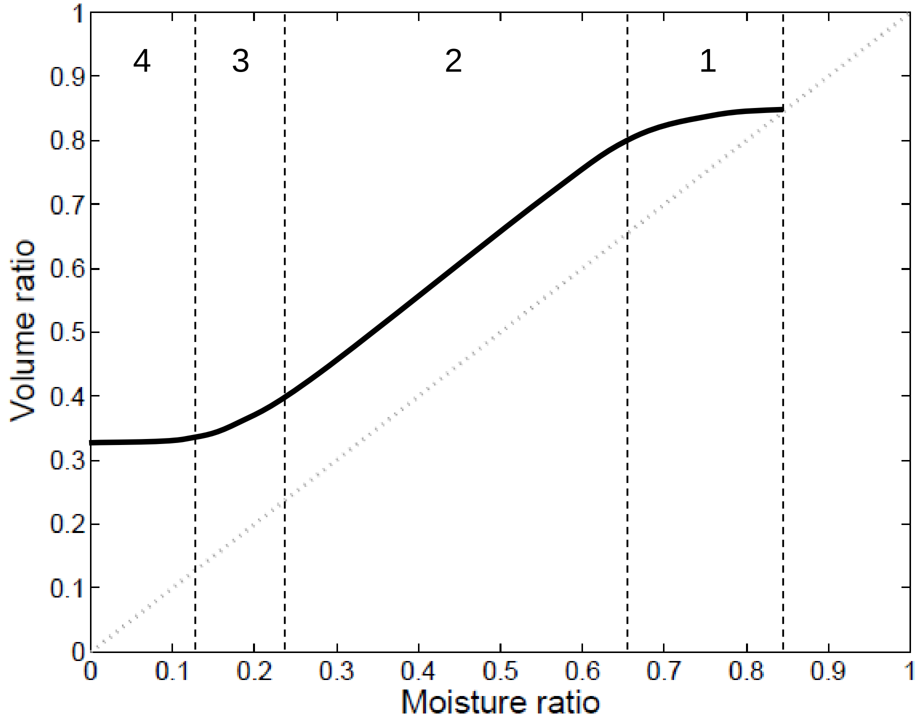

Fig. 1. Theoretical soil shrinkage characteristic curve, including 4 shrinkage phases.

HESSD
9, 13117–13154, 2012

Fig. 2. Google Earth image of the measurement area.

HESSD
9, 13117–13154, 2012

Storage change estimation from clay shrinkage

B. te Brake et al.

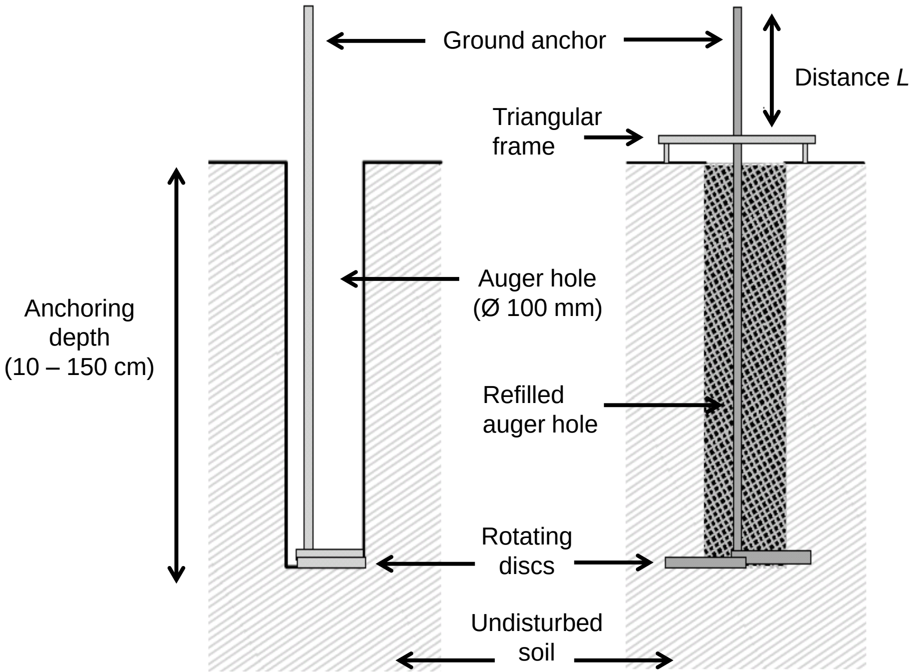

Fig. 3. Side view of the placement of ground anchors in the soil. Left: ground anchor lowered in augerhole. Right: ground anchor in refilled augerhole, with discs fixed in undisturbed soil after rotating the rod, and a metal frame placed over the rod.

HESSD
9, 13117–13154, 2012
Storage change estimation from clay shrinkage
B. te Brake et al.

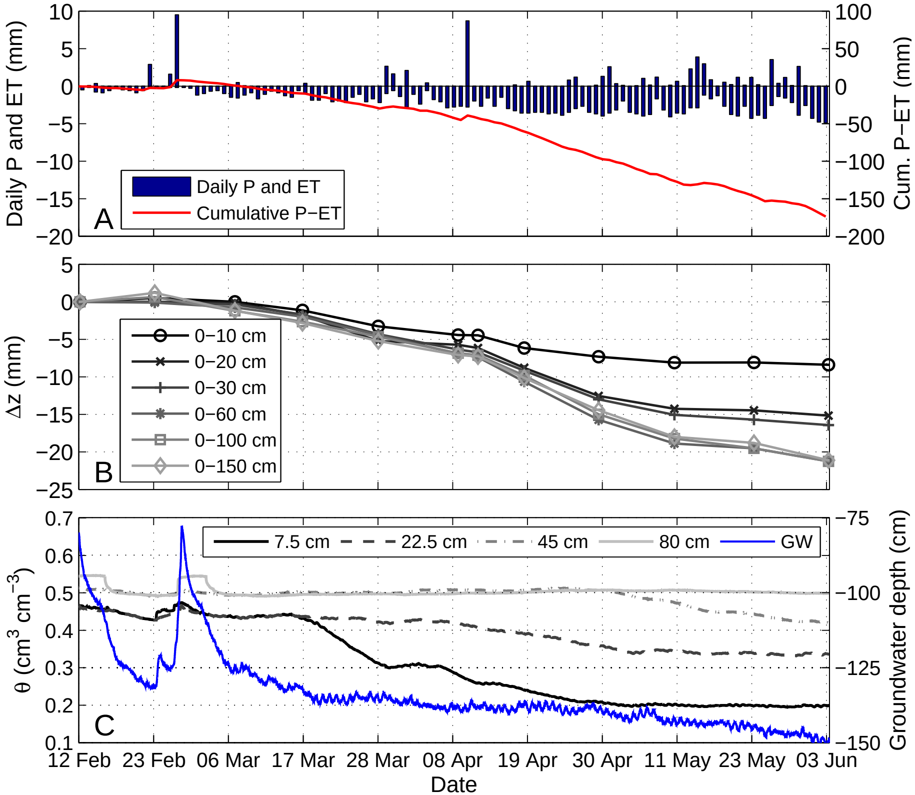

Fig. 4. Daily precipitation, daily evapotranspiration and cumulative net precipitation **(A)**, cumulative layer thickness change Δz in six soil layers with respect to the starting date **(B)**, volumetric soil moisture content θ from CS616 sensors at four depths and groundwater depth **(C)** at field A from 12 February until 3 June 2011.

HESSD

9, 13117–13154, 2012

Storage change estimation from clay shrinkage

B. te Brake et al.

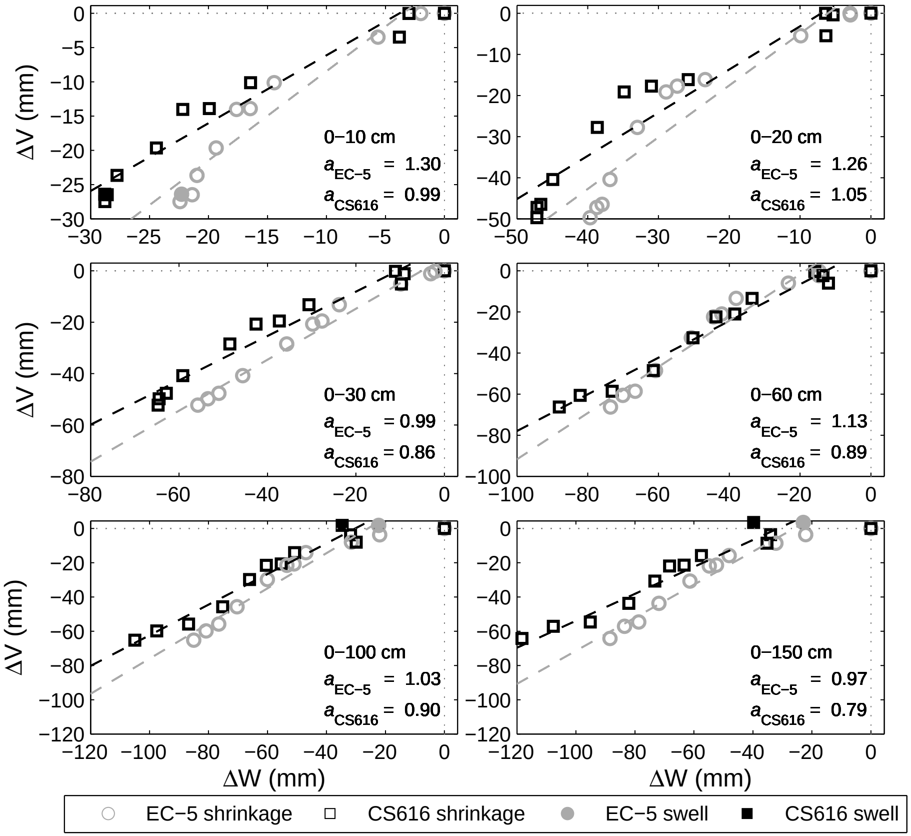

Fig. 5. Relationship between volume change per unit area ΔV and water storage change ΔW (EC-5 and CS616) at field A in 2011, for six soil layers. Dashed lines represent linear regression fits through data points outside the structural shrinkage phase, with a indicating the slope of the fit.

HESSD
9, 13117–13154, 2012

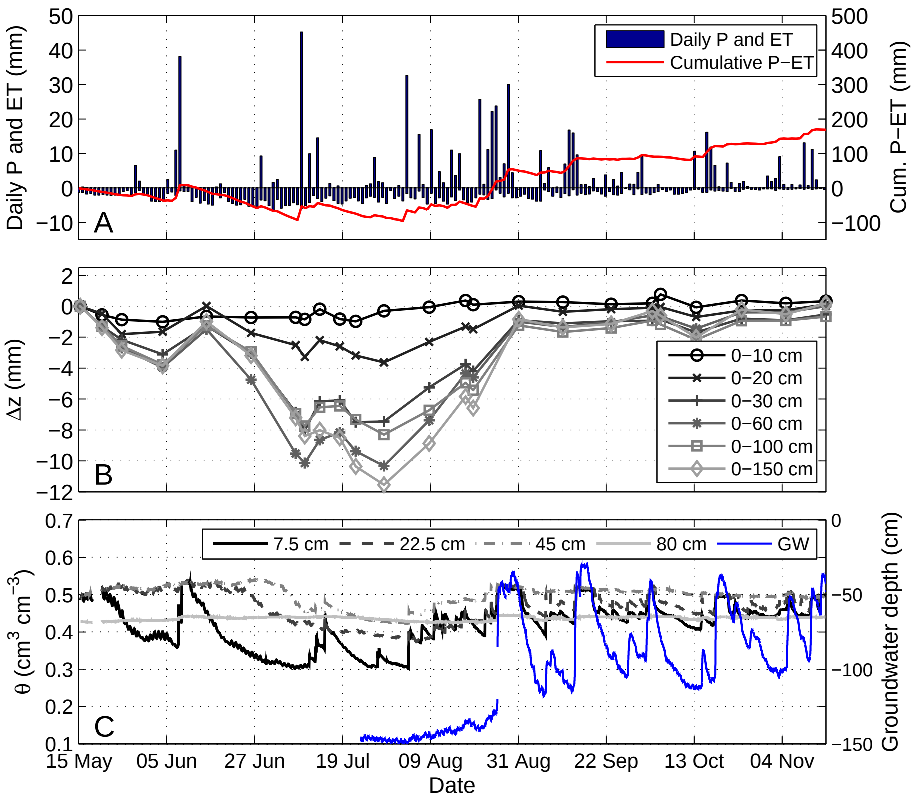

Fig. 6. Daily precipitation, daily evapotranspiration and cumulative net precipitation **(A)**, cumulative layer thickness change Δz in six soil layers with respect to the starting date **(B)**, volumetric soil moisture content θ from CS616 sensors at four depths and groundwater depth **(C)** at field B from 15 May until 15 November 2010. N.B. Soil moisture data logging failed between 18 May and 20 May, groundwater level measurements started at 22 July.

HESSD
9, 13117–13154, 2012

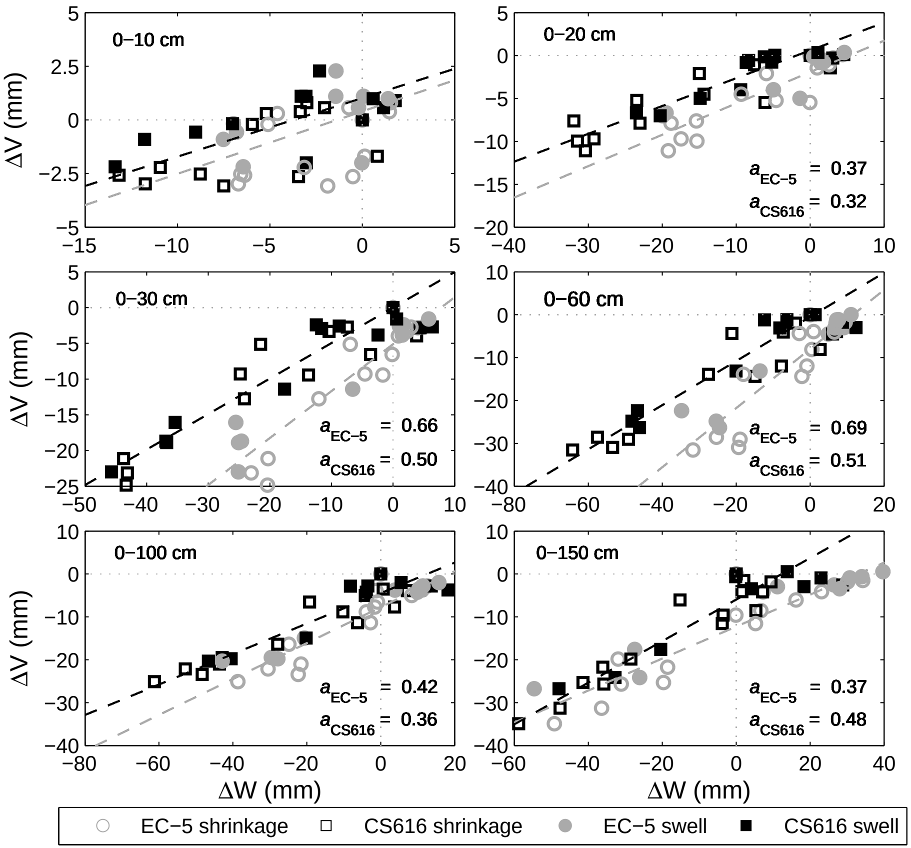

Fig. 7. Relationship between volume change per unit area ΔV and water storage change ΔW (EC-5 and CS616) at field B in 2010, for six soil layers. Dashed lines represent linear regression fits through data points outside the structural shrinkage phase. N.B. Slopes a for fits with $R^2 \geq 0.80$ are printed. Note the difference between the X and Y-axes.

HESSD
9, 13117–13154, 2012